Transcriptional adaptation to Clcn5 knockout in proximal tubules of mouse kidney

Jerry Wright, Marcelo M. Morales, Jackson Sousa-Menzes, Debora Ornellas, Jennifer Sipes, Yan Cui, Isabelle Cui, Phuson Hulamm, Valeriu Cebotaru, Liudmila Cebotaru, William B. Guggino and Sandra E. Guggino

Physiol. Genomics 33:341-354, 2008. First published 18 March 2008;
doi:10.1152/physiolgenomics.00024.2008

Physiological Genomics publishes results of a wide variety of studies from human and from informative model systems with techniques linking genes and pathways to physiology, from prokaryotes to eukaryotes. It is published quarterly in January, April, July, and October by the American Physiological Society, 9650 Rockville Pike, Bethesda MD 20814-3991. ISSN: 1094-8341, ESSN: 1531-2267. Visit our website at http://www.the-aps.org/.

Physiol Genomics 33: 341–354, 2008.
First published March 18, 2008; doi:10.1152/physiolgenomics.00024.2008.

Transcriptional adaptation to Clcn5 knockout in proximal tubules of mouse kidney

Jerry Wright,[1] Marcelo M. Morales,[2] Jackson Sousa-Menzes,[2] Debora Ornellas,[2] Jennifer Sipes,[3] Yan Cui,[3] Isabelle Cui,[3] Phuson Hulamm,[3] Valeriu Cebotaru,[3] Liudmila Cebotaru,[3] William B. Guggino,[2] and Sandra E. Guggino[1,3]

Departments of [3]Medicine and [1]Physiology, Johns Hopkins School of Medicine, Johns Hopkins University, Baltimore, Maryland; and [2]Instituto de Biophysica Carlos Chagas, Universidade Federal do Rio de Janeiro, Rio de Janeiro, Brazil

Submitted 28 January 2008; accepted in final form 13 March 2008

Wright J, Morales MM, Sousa-Menzes J, Ornellas D, Sipes J, Cui Y, Cui I, Hulamm P, Cebotaru V, Cebotaru L, Guggino WB, Guggino SE. Transcriptional adaptation to Clcn5 knockout in proximal tubules of mouse kidney. *Physiol Genomics* 33: 341–354, 2008. First published March 18, 2008; doi:10.1152/physiolgenomics.00024.2008.— Dent disease has multiple defects attributed to proximal tubule malfunction including low-molecular-weight proteinuria, aminoaciduria, phosphaturia, and glycosuria. To understand the changes in kidney function of the Clc5 chloride/proton exchanger gene knockout mouse model of Dent disease, we examined gene expression profiles from proximal S1 and S2 tubules of mouse kidneys. We found many changes in gene expression not known previously to be altered in this disease. Genes involved in lipid metabolism, organ development, and organismal physiological processes had the greatest number of significantly changed transcripts. In addition, genes of catalytic activity and transporter activity also had a great number of changed transcripts. Overall, 720 genes are expressed differentially in the proximal tubules of the Dent Clcn5 knockout mouse model compared with those of control wild-type mice. The fingerprint of these gene changes may help us to understand the phenotype of Dent disease.

gene array; Dent disease; cholesterol; endocytosis

DENT DISEASE, an X-linked renal tubular disorder, is characterized by low-molecular-weight proteinuria, aminoaciduria, glycosuria, phosphaturia, hypercalciuria, nephrolithiasis, and progressive renal failure (38). The etiology of X-linked Dent disease 1 is established to be due to mutations of the CLCN5 gene (13, 25, 49). Previous studies by our group (7, 39, 46) established that a Clcn5 knockout mouse (Clcn5 KO) is a model that has all of the renal attributes of Dent disease including Fanconi syndrome, hypercalciuria, nephrocalcinosis, and renal failure. Another Clcn5 KO mouse made by the Jentsch group has some of the features of Dent disease but not others (14).

The previous studies of the Willnow and Jentsch groups used gene arrays on whole kidney from the megalin knockout and Jentsch Clcn5 KO mice. These revealed 21 and 58 changes in gene expression, respectively (23, 29). We wondered whether this may be due to the fact that contamination from medullary thick ascending limb cells and collecting ducts as well as other tubules in the cortex including distal tubules, collecting ducts, or vascular tissue would blunt changes attributed to the proximal tubule. Therefore, the goal of this gene array was to determine what adaptations occur in the genes of the proximal tubules after a knockout of Clcn5. By isolating proximal tubules, we hypothesized that the gene profile might give some hint as to the underlying molecular compensations that occur from the knockout of Clcn5 in that tubule. We found that numerous genes of biological process or molecular function had changes in mRNA. This gene array shows that there may be substantial, heretofore unexpected changes in metabolism in the proximal tubule of these Clcn5 knockout mice.

CLC5 is a proton/chloride exchanger (37) expressed in renal tubules including the thick ascending limb and the cortical collecting ducts, but the highest expression is in the proximal tubule (12). Clc5 is found in the early endosome, where it is thought to help acidify the endosomal compartment in conjunction with H^+-ATPase (12, 15, 28). Thus Clc5 provides the counterion, chloride, for proton movement across the endosomal membrane. It has already been found that a lack of Clc5 causes several important changes in transporters of the kidney of the Clcn5 KO (34). These changes are thought to occur because the early endosomal compartment, which is involved in trafficking of proteins from the apical membrane, has an increased pH in the Clcn5 KO. For example, in the Clcn5 KO, megalin, cubulin, the sodium/proton exchanger Slc9a3 (Nhe3), and the sodium-phosphate cotransporter Slc34a1 (Npt2a) are situated off of the plasma membrane in an intracellular compartment (10). One goal of this gene array, therefore, was to try to shed light on the causes of this altered distribution of transporters by determining whether genes that control trafficking, endosome function, or ion transport are altered in expression level.

We previously found (39) that the Guggino Clcn5 KO, like human Dent disease patients not in renal failure, has twofold elevated 1α,25-dihydroxyvitamin D_3 compared with wild-type mice (WT), even though vitamin D binding protein (DBP) is lost as part of the low-molecular-weight proteinuria. The Guggino Clcn5 KO does not have a serum parathyroid hormone (PTH) level that is different from WT (39). Therefore, the Guggino Clcn5 KO appears to mimic Dent disease patients, who usually have normal or slightly lowered PTH levels (38). Although the Jentsch mouse and Guggino mouse models both lack mRNA and protein for Clcn5 and both mice have a similar knockout strategy that causes disruption of Clcn5 at the pore region, the Jentsch ClCn5 KO has low levels of 1α,25-dihydroxyvitamin D_3, thought to be due to urinary loss of DBP (34). Lowered serum 1α,25-dihydroxyvitamin D_3 is also found in the megalin knockout mouse, which also loses DBP into the urine because megalin, the receptor for DBP uptake, is absent (23). What causes the different outcomes of serum 1α,25-dihydroxyvitamin D_3 in these three mice? Can gene array

Article published online before print. See web site for date of publication (http://physiolgenomics.physiology.org).

Address for reprint requests and other correspondence: S. E. Guggino, 929 Ross Bldg., 720 Rutland Ave, Johns Hopkins Univ., Baltimore, MD 21205 (e-mail: sguggino@jhmi.edu).

determine what compensations occur in the ClCn5 KO model compared with WT?

The gene array performed by the Jentsch group on Clcn5 KO (29) found that there was an eightfold decreased mRNA for the 1α,25-dihydroxyvitamin D_3 24-hydroxylase (Cyp24a1). When the conversion of 1α,25-dihydroxyvitamin D_3 to 1α,24,25-trihydroxyvitamin D_3 occurs, the less potent 24-hydroxylated by-product has a much reduced binding to the vitamin D receptor. Thus transcription of 1α,25-dihydroxyvitamin D_3-dependent genes is decreased. But a decrease in Cyp24a1 would cause a slowed conversion of the active hormone 1α,25-dihydroxyvitamin D_3 to the inactive form 1α,24,25-trihydroxyvitamin D_3, thus acting to maintain levels of 1α,25-dihydroxyvitamin D_3. Lowered mRNA of Cyp24a1 was also documented in the megalin knockout mouse (29).

The Jentsch gene array also indicated that the mRNA of 25-hydroxyvitamin D_3 1α-hydroxylase (Cyp27b1) was about fourfold elevated (29). This result was not found in the megalin knockout mouse. Although changes in this hydroxylase would be predicted to increase the levels of 1α,25-dihydroxyvitamin D_3, the actual level of serum 1α,25-dihydroxyvitamin D_3 was lowered in the Jentsch Clcn5 KO and megalin knockout mouse models, but not the Guggino Clcn5 KO model. The Jentsch gene array also found that the mRNA of several proteins, which are transcriptionally regulated by 1α,25-dihydroxyvitamin D_3 through the vitamin D receptor, were upregulated. These included TrpV6 (ECac2) and calbindin D_{28K} in the kidney, but not calbindin D_{9K} or TrpV5 (ECac1) in the intestine. Thus, although the absolute level of serum 1α,25-dihydroxyvitamin D_3 was low, the kidney, but not intestinal, mRNA levels of target genes were increased. Maritzen et al. (29) propose a model that explains the results of these outcomes. The Guggino group (39) found previously that the mRNA of both the intestinal genes calbindin D_{9K} and TrpV5 (ECac1) were increased as measured by Northern blot. This result is expected because the Guggino Clcn5 KO mice have higher serum 1α,25-dihydroxyvitamin D_3 than WT (39). Because of the importance of Cyp27b1 to calcium balance, we measured protein levels of this enzyme.

METHODS

Tubule RNA and protein. Mice were killed with halothane according to protocols approved by the Animal Care and Use Committee at Johns Hopkins Medical School. Renal proximal tubules were dissected from cortical slices. At the glomerulus the first 1–1.5 mm of tubule was designated the S1 segment and the next 1–1.5 mm the S2 segment. The S1 and S2 segments were in equal abundance. This dissection and the mRNA extraction were preformed as previously described (33, 41, 52). To isolate tubular RNA, the abdominal aorta was accessed and the left kidney was perfused with an ice-cold salt solution containing (in mM) 135 NaCl, 5 KCl, 1.0 $Na_2PO_4 \cdot 7H_2O$, 3.0 sodium acetate, 1.2 $NaSO_4$, 2.5 $CaCl_2$, 1.2 $MgSO_4$, 5 HEPES, and 5.5 glucose, with 1× RNase inhibitor, in diethyl pyrocarbonate (DEPC)-treated water adjusted to pH 7.4 (all reagents were from Sigma). The salt solution was followed by perfusion with a digestion solution, which was the above salt solution supplemented with 0.125 mg/ml collagenase B (Worthington) and 0.1% bovine serum albumin (BSA; Sigma). The left kidney was dissected into fine transverse slices and incubated at 37°C for 30 min in digestion solution with continuous shaking. Proximal tubule dissection was performed under a dissecting microscope in an ice-cold salt solution. The proximal tubules were placed in prechilled Eppendorf tubes containing 800 μl of chilled TRIzol reagent (Invitrogen). The tubules were homogenized immediately upon dissection (~10 min) with a tissue homogenizer (Kontes Glass, Vineland, NJ) designed for Eppendorf tubes. RNA was isolated according to the TRIzol protocol (GIBCO BRL, Gaithersburg, MD). After dissection of ~80–100 segments of 2-mm length per kidney, the RNA from three or four mice was combined to have enough RNA per chip. Three chips were used for each of wild-type and knockout samples.

After the ethanol precipitation step in the TRIzol extraction procedure, the RNA was purified with the Qiagen RNeasy Total RNA isolation kit. Quantification of the RNA yield was assessed by spectrophotometric analysis. Absorbance (A) was checked at 260 and 280 nm for determination of sample concentration and purity. The A_{260}-to-A_{280} ratio was between 2.0 and 2.1. The total RNA had a concentration of 0.8–1 μg/μl, in order to obtain sufficient quantity of labeled cRNA for hybridization on the GeneChip expression probe arrays. The cDNA synthesis protocol was performed with 7.5 μg of total RNA as starting material. Double-stranded cDNA was synthesized, and then the biotin-labeled cRNA was generated and fragmented for target hybridization. The washing, staining, and scanning of probe arrays was performed according to Affymetrix sample preparation procedures as outlined in the Affymetrix GeneChip Expression Analysis Technical Manual (no. 701021 rev. 2). The hybridization was performed in the Johns Hopkins Gene Array Center.

The RT-PCR reaction was performed with a program of 94°C for 45 s, 60°C for 45 s, 52–62°C for 45 s, 72°C for 45 s, using 32–36 cycles. RT-PCR primer sequences were taken from the hybridized sequences of genes on the MOE 430A gene chip. These sequences and their annealing temperatures are Angpt1 (59): 1424485_AT, forward attcaacaccggaaagatgg, reverse tccctttgctctgtgattcc; Gc (60): 1426547_AT, forward cagctgctgaaccacttcaa, reverse accatggaggatttctgtcg; F5 (60): 1449269_AT, forward aacggatgttccacaccact, reverse accatggagaggatttctgtcg; Gucyla3 (62): 1434141_AT, forward tcatcctcttaagctgtgcagt, reverse ggaaccgtacatggagcttcta; Hmgcs2 (52): 1423858_A_AT, forward cccctgaggaattcacagaa, reverse tctccattagacgggacacc; Clcn5 (59): 1429400_AT, forward cagcatcttggtcatgtcac, reverse ggctactgcgactgaagc; Cxc11 (59): 1419209_AT, forward gcacctgtctggtgaacg, reverse ccacacatgtcctcaccc; Gadd45g (52): 1453851_A_AT, forward tggtctgatcgacttggtga, reverse cagtcggctaagtccagctc; NT5e (59): 1428547_AT, forward gtcctgtgaccaagtgagca, reverse ccttatttactcgccaagca; and Scl10a2 (59): 1450245_AT, forward caaccagatgagaagtag, reverse gaggcttaagcttctgtg.

To isolate proximal tubule protein, the kidney was first perfused with Hanks' balanced salt solution containing a cocktail tablet of protease inhibitors (Roche Diagnostics), followed with the protease solution containing collagenase B. Tubules were incubated with collagenase B and then isolated by dissection in the protease solution on ice. Groups of tubules were pooled from four or five mice and then homogenized in Eppendorf tubes in RIPA buffer (52). Western blots of tubules or kidney cortex were performed as previously described (47). The antibody for Cyp27b1 was from H. J. Ambrecht (St. Louis VA Medical Center, St. Louis, MO). The antibody for NHE10/sperm was from Dan Wang (University of Texas Southwestern, Dallas, TX). The antibody for Cap 1 was from E. Bertling and P. Lappalainen (University of Helsinki, Helsinki, Finland). The antibody to Slc10a2 was from P. A. Dawson (Wake Forest University, Winston-Salem, NC).

Quality control measures. After scanning, array images were assessed by eye to confirm scanner alignment and the absence of significant bubbles or scratches. The 3′-to-5′ ratio for GAPDHMur was confirmed to be <2 for all six chips used in the analysis. The spike controls BioB, BioC, BioD, and CreX were identified as being present in increasing intensity. GeneChip initial expression analysis was performed with GCOS 1.2 software (Affymetrix, Santa Clara, CA).

Microarray data analysis. GeneChip expression data were exported to GeneSpring 7.2 (Silicon Genetics, Redwood City, CA), where per-chip normalization to the 50th percentile expression level and per-gene normalization to the median expression intensity in all

samples was performed. Only probe sets scored as present or marginal in at least 50% of samples were included in the analysis. Data were transformed to log ratio for display and analysis. GeneSpring and S-Plus 6.2 (MathSoft, Cambridge, MA) software programs were used in data analysis and visualization. A candidate list of genes was produced by setting $P \leq 0.05$ with the GeneSpring *t*-test with the cross-gene error model activated, which uses the Rocke-Lorenzato model of error correction (36). The filtered gene list was further refined by submitting it to ANOVA analysis using a false discovery rate (FDR) (4) cutoff of 10%. This was similar to the results from Statistical Analysis of Microarrays (43) with 10% FDR, with an 80% overlap with ANOVA results.

Those probe sets identified as significantly differentially expressed by genotype underwent an intensive search to identify biological function. Probe set sequences from the Affymetrix web site were checked against the University of California, Santa Cruz genome database to verify identity and update annotation. For individual genes with multiple probe set sequences specific to different regions of the gene, each probe set was checked separately. The resulting list of genes was submitted to PathwayAssist 3.0 (Stratagene, La Jolla, CA) for automated literature search. Gene Ontology (GO) (3) classifications using GOMiner, conserved protein family domains, and reference literature were used to construct functional groupings of genes. GOMiner was utilized to perform a two-sided Fisher's exact test to determine whether a significantly greater number than expected of differentially expressed genes occurred in a GO category (50). Gene identity was also documented with all of the NIH databases including OMIM, PubMed, etc. All original array data images and files are available online at NCBI.

RESULTS

With the MOE 430 Plus 2 Affymetrix array chips, 45,101 probe sets were interrogated and 21,194 of these sets were scored as present or marginal in at least 50% of dissected proximal tubule samples from Clcn5 KO ($n = 3$ chips) and WT ($n = 3$ chips). ANOVA analysis using a Benjamini and Hochberg FDR multiple testing correction of 10% discovered 963 significantly changed candidate probes representing 720 uniquely named genes or expressed sequence tags (ESTs).

RT-PCR validation was performed on some genes of increased and decreased expression. Slc10a2 mRNA expression was 17-fold elevated in Clcn5 KO vs. WT proximal tubules in the gene array and showed a sixfold increase by RT-PCR. Gadd45g mRNA was upregulated by 2.75-fold in Clcn5 KO vs. WT in the gene array and 1.8-fold in the RT-PCR experiments. Likewise, 5′-nucleotidase showed a 2.5-fold upregulation by gene array and 1.7-fold by RT-PCR. The gene transcripts downregulated in the gene array in Clcn5 KO vs. WT are Hmgcs2 (−12.5), Clcn5 (−7.14), F5 (−4.54), and Gucyla3 (−2.22) and these were −2.86, −2.86, −1.67, and −1.67, respectively, by RT-PCR. The RT-PCR mRNA changes were indicative of changes in transcripts recorded by the gene array.

In preliminary gene array studies of the whole kidney, an Affymetrix MOE 430 gene array chip was used to determine the level of expression of genes; we found that Clc5 in the Clcn5 KO kidney was 2.8-fold lower compared with WT kidney. The ratio found by Jentsch with the Affymetrix U74v2 array and the whole kidney (Clcn5 KO/WT) was 1.2-fold decreased (29). We found that 45 gene transcripts were significantly different in preliminary screens of whole kidney from Clcn5 KO and WT. Besides Clcn5, only one gene was common to the Jentsch whole kidney gene array and this was midkine, a gene that did not show a significant change in our proximal tubule array (Supplemental Table S1).[1] As a first investigation of the gene array sensitivity to tissue source, we looked at the ratios of Clcn5 mRNA in the dissected proximal tubules by comparing Clcn5 KO and WT. Using the Affymetrix 430 Plus 2 array, we found that Clcn5 expression was reduced an average of fourfold across four probe sets. This validated that the MOE 430 Plus 2 gene arrays were sensitive to decreases in the mRNA for Clcn5 in proximal tubules. Because few genes were changed in whole kidney, the apparent decrease in the Clcn5 abundance seemed larger with proximal tubules; we used these for gene array analysis. We believe the more uniform proximal tubule preparation contributes to the sensitivity of this array.

From GOMiner analysis, Table 1 shows the groups significantly changed in the biological process category. The top significantly changed groups were (changed/total, *P* value) *1*) lipid metabolism (37/255, <0.0001), *2*) organ development (36/402, 0.014), *3*) organismal physiological process (36/433, 0.04); *4*) cellular lipid metabolism (which has many of the same changes as those in the lipid metabolism category) (30/220, <0.0001), *5*) organic acid metabolism (29/217, 0.0001), and *6*) ion transport (26/270, 0.016). Also notable were the changes in metal ion transport (16/142, 0.014), steroid metabolism (10/64, 0.006), lipid transport (7/31, 0.002), cholesterol metabolism (5/31, 0.04), and vitamin D metabolism (3/4, 0.0009). Categories that were not significantly changed in the biological process summary included phosphate or phosphorus metabolism, intracellular signaling (cell-surface receptor-linked signal transduction), and metal ion binding for iron, zinc, and copper (data not shown).

The class with the greatest number of changes in gene transcript level, lipid metabolism, was surprising because overall changes in lipids have not been reported in Dent disease. This class had changes in 37 genes including Mte1, Pld1, Osbp13, Mapk14, Ipl, Hpgd, Apoc3, Adfp, Facl4, Hmgcs2, Facl3, Acaa1, Amacr, Hexa, Tbxas, Hsd11b1, Srd5a2, Dhrs8, Hsd3b4, Abca1, Pip5k2b, Pte2a, Hmgcs1, Dci, Lpin1, Bucs1, Vldlr, Cpt2, Cte1, Slc27a1, Galc, Mgll, Acaa2, Lip1, Facl2, Hdlbp, and Angptl3. Only five genes (Hmgcs1, Lpin1, Dhrs8, Amacr, and Apoc3) increased in expression; the rest were decreased in expression. The changes in lipid metabolism transcripts are found mainly in genes of fatty acid, sterol, and cholesterol metabolism, which we divided into subgroups for easier analysis.

In fatty acid metabolism significantly changed transcripts (15/73) were Mte1, Pld1, Osbp13, Mapk14, Ipl, Hpgd, Apoc3, Adfp, Facl4, Hmgcs2, Facl3, Acaa1, Amacr, Hexa, Tbxas, Hsd11b1, Srd5a2, Dhrs8, Hsd3b4, Abca1, Pip5k2b, Pte2a, Hmgcs1, Dci, Lpin1, Bucs1, Vldlr, Cpt2, Cte1, Slc27a1, Galc, Mgll, Acaa2, Lip1, Facl2, Hdlbp, and Angptl3. The fatty acid long chain coenzyme A ligase, Facl3, which utilizes myristate, laurate, arachidonate, and eicosapentaenoate (−1.92, −1.67), and fatty acid coenzyme A ligase 2 (Facl2), which acts on shorter-chain fatty acids (−1.92) are downregulated. The cytosolic acyl-CoA thioesterase Cte1 (−2.27) and the long-chain fatty acid transporter Slc27a1 (−1.67) are also downregulated. The gene with the lowest fold expression is Mte1 or Acot2 (−2.27), a mitochondrial acyl-CoA thioesterase.

[1] The online version of this article contains supplemental material.

Table 1. *Gene Ontology: biological processes*

GO ID	Total	Changed	*P* Value	Term
6629	255	37	<0.0001	Lipid metabolism
48513	402	36	0.0147	Organ development
50874	433	36	0.0401	Organismal physiological process
44255	220	30	<0.0001	Cellular lipid metabolism
6082	217	29	0.0001	Organic acid metabolism
19752	217	29	0.0001	Carboxylic acid metabolism
6811	270	26	0.0156	Ion transport
9887	226	22	0.0223	Organ morphogenesis
9605	131	17	0.0028	Response to external stimulus
30001	142	16	0.014	Metal ion transport
6807	156	16	0.0311	Nitrogen compound metabolism
6631	73	15	<0.0001	Fatty acid metabolism
9308	145	15	0.0339	Amine metabolism
6519	124	14	0.0204	Amino acid and derivative metabolism
6066	111	12	0.0408	Alcohol metabolism
7610	85	11	0.015	Behavior
9611	97	11	0.0363	Response to wounding
6520	98	11	0.0388	Amino acid metabolism
7626	52	10	0.0011	Locomotory behavior
8202	64	10	0.0055	Steroid metabolism
42592	79	10	0.023	Homeostasis
16042	35	8	0.0011	Lipid catabolism
6869	31	7	0.0024	Lipid transport
45595	50	7	0.0328	Regulation of cell differentiation
6725	51	7	0.0361	Aromatic compound metabolism
6935	29	6	0.0076	Chemotaxis
42330	29	6	0.0076	Taxis
8652	23	5	0.0118	Amino acid biosynthesis
7596	28	5	0.0267	Blood coagulation
44271	29	5	0.0307	Nitrogen compound biosynthesis
50817	29	5	0.0307	Coagulation
9309	29	5	0.0307	Amine biosynthesis
7599	29	5	0.0307	Hemostasis
8203	31	5	0.0397	Cholesterol metabolism
9968	32	5	0.0447	Negative regulation of signal transduction
45444	12	4	0.0048	Fat cell differentiation
9069	14	4	0.0088	Serine family amino acid metabolism
45597	20	4	0.0317	Positive regulation of cell differentiation
48511	22	4	0.0435	Rhythmic process
42359	4	3	0.0009	Vitamin D metabolism
6637	6	3	0.0041	Acyl-CoA metabolism
6563	7	3	0.0068	L-Serine metabolism
42593	7	3	0.0068	Glucose homeostasis
19395	10	3	0.0204	Fatty acid oxidation
6775	11	3	0.0267	Fat-soluble vitamin metabolism
44242	12	3	0.034	Cellular lipid catabolism
30217	12	3	0.034	T cell differentiation
45408	3	2	0.011	Regulation of interleukin-6 biosynthesis
42226	3	2	0.011	Interleukin-6 biosynthesis
19377	4	2	0.0211	Glycolipid catabolism
46068	4	2	0.0211	cGMP metabolism
45582	4	2	0.0211	Positive regulation of T cell differentiation
6544	4	2	0.0211	Glycine metabolism
1676	4	2	0.0211	Long-chain fatty acid metabolism
6182	4	2	0.0211	cGMP biosynthesis
31649	4	2	0.0211	Heat generation
48005	4	2	0.0211	Antigen presentation, exogenous peptide antigen
43154	4	2	0.0211	Negative regulation of caspase activity
30317	4	2	0.0211	Sperm motility
45580	5	2	0.0337	Regulation of T cell differentiation
1892	5	2	0.0337	Embryonic placenta development
6564	5	2	0.0337	L-Serine biosynthesis
1659	5	2	0.0337	Thermoregulation
48002	5	2	0.0337	Antigen presentation, peptide antigen
1890	6	2	0.0485	Placenta development
42591	6	2	0.0485	Antigen presentation via MHC class II
19915	6	2	0.0485	Sequestering of lipid
19886	6	2	0.0485	Antigen processing via MHC class II
30149	6	2	0.0485	Sphingolipid catabolism

Because GOMiner analyzes lists of descriptions that are hand curated and does not address relationships among categories, analysis was extended by mapping the Kyoto Encyclopedia of Genes and Genomes (KEGG) pathways to the significantly changed gene list. Additional gene transcripts in the fatty acid metabolism pathway were also found to be decreased in Clcn5 KO vs. WT proximal tubules. These include acetyl-coenzyme A acyl transferase (−1.35), 3-ketacyl-CA thiolase (−1.33), acetyl-coenzyme A acyltransferase 2 (mitochondrial 3-oxoacyl-coenzyme A thiolase) (−1.56), and dodecenoyl-coenzyme A δ isomerase (−1.43), which are all decreased. Carnitine palmitoyltransferase 2 (Cpt2), which catalyzes the last step of fatty acid entry to mitochondria, is also decreased (−1.45). Cyp4a10 (−3.57) and Cyp4a14 (−33.3), which are involved in the metabolism of fatty acids and eicosanoids, are also decreased. One gene transcript in this pathway that is upregulated is aldehyde dehydrogenase (mitochondrial) (1.34). As a group these KEGG pathway gene changes are significant to 7.2E−09.

In the subclass of steroid metabolism 10 of 64 gene transcripts are significantly changed; these are Vldlr, Osbpl3, Hsd11b1, Srd5a2, Hmgcs1, Hdlbp, Dhrs8, Hsd3b4, Hmgcs2, and Abca1. The mRNA with the largest increase is 3-hydroxy-3-methylglutaryl (HMG)-CoA synthase 1 (Hmgcs1) (1.8). The protein for Hmgcs1 is a transcriptionally regulated enzyme of cholesterologenesis. The next gene, oxysterol binding protein-like 3 (Osbpl3), has transcripts increased 1.6-fold. The gene with the lowest transcript expression in steroid metabolism is HMG-CoA synthase 2 (Hmgcs2) (−12.5). The cholesterol efflux pump Abca1 transcripts are also decreased (−1.56) in Clcn5 KO proximal tubules compared with WT.

In the subclass of cholesterol metabolism (5/31), a number of key metabolic enzyme transcripts, including Vldlr, Hmgcs1, Hdlbp, Hmgcs2, and Abca1, are changed in Clcn5 KO vs. WT mice. Other cholesterol gene transcripts that were significantly changed but not included in this subclass include the ATP citrate lyase, which makes cellular acetyl-CoA in many tissues (10-fold). Acetyl-CoA is involved in several important biosynthetic pathways including cholesterologenesis. The rate-limiting enzyme in cholesterol synthesis, squalene monooxygenase, has a twofold increase in transcript expression. Cytoplasmic HMG-CoA synthase 1 (Hmgcs1), which mediates an early step in cholesterol synthesis, is upregulated in transcript level (1.84). Glucose-6-phosphate dehydrogenase is a key enzyme in the pentose phosphate pathway that is involved in providing reducing equivalents (NADPH) for biosynthesis of fatty acids and cholesterol. This enzyme transcript is up 1.6-fold in the Clcn5 KO proximal tubules compared with the WT proximal tubules. Abca1, a member of the ATP-binding cassette (ABC)-transporter family, is downregulated (−1.5); apolipoproteins are also decreased (−1.56-fold). It remains to be tested whether these changes in lipid, sterol, or cholesterol metabolism cause any changes in the Dent phenotype, in particular in endocytosis.

Because this disease is accompanied by significant changes in transport function, we paid particular attention to this class of genes. In the class of ion transport genes (26/270) many genes show changes in transcripts, including Atp10d, Atp6v1e, Ftl1, Kcnk5, F5, Scl03a1, Atp4a, Slc4a1, Slc10a2, Slc38a3, Slc26a7, Slc34a3, Mcoln1, Adrb2, Atox1, Cp, Slc30a7, LOC20816, Kcne1, Gabrb3, Pln, Slc39a8, Clcn5, Slc8a1, Moat6, and Clcn3. The gene expression transcripts that are most highly upregulated are the Asbt solute carrier or Slc10a2. This gene mRNA is upregulated 17-fold in the Clcn5 KO mouse proximal tubules compared with WT. This gene was also highly expressed in KO whole kidney (8-fold) compared with WT (Supplemental Table S1). Absorption of a bile analog, cholylsarcosine, which is absorbed on this transporter, was shown to increase when 1α,25-dihydroxyvitamin D_3 was given. The activation of Slc10a2 by 1α,25-dihydroxyvitamin D_3 is abrogated after site-directed mutagenesis or deletion of the vitamin D response element (VDRE) in the Slc10a2 (ASBT) promoter (8). The increase in this transcript may be caused by increased levels of serum 1α,25-dihydroxyvitamin D_3 in the Guggino Clcn5 KO mouse. However, this protein is not increased significantly, suggesting further regulation at another level (Fig. 1). In the Jentsch gene array this transcript was decreased 69% compared with WT, which could reflect the lowered 1α,25-dihydroxyvitamin D_3 in that mouse. Clcn3 transcripts are also upregulated in the Clcn5 KO tubules, as shown by four different probe sets of the gene (1.94, 1.79, 1.71, 1.69). Whether the Clc3 channel protein is upregulated in the Clcn5 KO is still unknown. The putative sodium/proton exchanger-like protein mRNA LOC208169 (NHE10/sperm) was downregulated (−2.17). The sodium/proton exchanger NHE10/sperm is thought to function by extruding protons from sperm, where lowered intracellular pH is a critical factor in sperm motility. NHE10/sperm has been found to target the plasma membrane of cells (45), where it acts functionally like a sodium/proton exchanger, but the physiology of NHE10/sperm in the kidney is not known. Western blotting shows that Nhe10/sperm is slightly decreased in Clcn5 KO proximal tubules compared with WT (data not shown), and cell fractionation shows that Nhe10 resides in the plasma membrane fraction because it localizes with the membrane marker aminopeptidase N (not shown).

Two other categories of interest in the physiology of Dent disease that are not significantly changed as a group but have individual significant changes in gene transcript levels are those of vesicle-mediated transport (8 genes: Mcoln1, Vldlr, Cav2, Stab2, Kdelr2, Cap1, Abca1, Clcn5) and endocytosis (6 genes: Vldlr, Cav2, Stab2, Cap1, Clcn5, Abac1). These two processes might be expected to change in Dent disease because

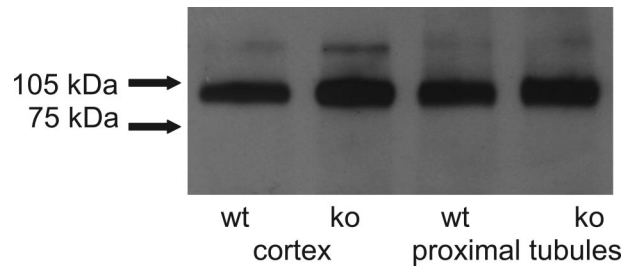

Fig. 1. Western blot of the bile salt transporter Slc10a2 in wild type (WT) or Clcn5 knockout (KO) kidney cortex or proximal tubules. A total of 15 μg of kidney cortex or proximal tubule was added to each lane. Primary antibody was used at 1/500 and secondary antibody at 1/5,000. This blot shows that protein expression of Slc10a2 is nearly identical in WT and KO even though the mRNA is 17-fold greater in the KO proximal tubules compared with WT. The increase at the gene transcript level in KO is probably a result of the increased circulating 1α,25-dihydroxyvitamin D_3 that has been shown to stimulate transcription of this gene. Posttranslational regulation must cause decreases in the protein. Representative of 3 studies.

there are megalin-mediated transport defects in low-molecular-weight protein uptake and changes in transporter trafficking that are associated with this disease. The gene with the highest expression in these two groups of vesicle transport/endocytosis genes is adenylate cyclase-associated protein 1 (Cap1) (9.0, 5.0). The Cap1 protein promotes actin filament depolymerization and is needed for the proper cellular localization of profilin (5). Cap1 has recently been shown to bind profilin directly (6). The endoplasmic reticulum protein retention receptor 2, Kdelr 2 (1.60), has a Lys-Asp-Glu-Leu motif that retains proteins in the endoplasmic reticulum. The increase in this gene mRNA if translated into protein would suggest that more proteins are kept in the endoplasmic reticulum in Clcn5 KO proximal tubules. Such a change might predict a more global decrease in protein trafficking than was previously thought. Caveolin 2 (Cav2) is also upregulated (1.41). Caveola formation and exit from the Golgi complex is associated with caveolin oligomerization in association with cholesterol (35). Caveolins are cholesterol-binding proteins involved in the regulation of several intracellular processes including cholesterol transport, signal transduction, and endocytosis and transcytosis (2). In MDCK cells, caveolin 2 localizes to the Golgi and the plasma membrane (32). The fact that caveolin 2 mRNA is up in the Clcn5 KO may mean increases in caveolin-mediated exo-/endocytosis. This, coupled with the fact that cholesterol metabolism is changed, may point to an increased caveolin-mediated endocytosis. This has not been explored at the protein level in this mouse at the present time. Rab escort protein 1 mRNA (1.6) is also upregulated. The Rab escort protein chaperones newly prenylated Rab proteins to their target membranes (1).

Downregulated gene transcripts in the classes of vesicle-mediated transport and endocytosis include synaptotagmin 1 (−1.43), which is a complexin/synaptotagmin 1 switch that controls fast synaptic vesicle exocytosis. The complexin proteins are fusion clamps. By arresting vesicle secretion just prior to fusion, complexin primes select vesicles for a fast, synchronous response to calcium (30). The gene for the very low-density lipoprotein receptor Vldlr (−1.41) is highly expressed in tissues that are active in fatty acid metabolism. Mice lacking either Reln or Vldlr and ApoER2 (42) exhibit a dramatic increase in the phosphorylation level of the microtubule-stabilizing protein tau. Stabilin-2 (Stab2) (−1.54) is part of a novel family of fasciclin domain-containing hyaluronan receptor homologs. Stabilins are present in early endosomal antigen (EEA)-1-positive organelles colocalizing with endocytosed BSA (17). The cholesterol efflux transporter Abca1 (−1.56) belongs to a group of traffic ATPases. Mutations in the ABCA1 gene cause Tangier disease, a disease of low serum high-density lipoprotein (HDL) (51). The membrane transporter ATP-binding cassette transporter A1 (ABCA1) has been shown to be the rate-limiting step in the initial formation of plasma HDL particles. The mechanisms of action of ABCA1, including its role in the vesicular transport of lipids to the cell surface for the lipidation of HDL apolipoproteins, are not fully understood.

Even though there were few genes associated with vitamin D_3 metabolism, they were significantly changed and are of interest for the changes in vitamin D_3 metabolism in this disease. The cytochrome *P*-450 Cyp24a1 mRNA is lowered in Clcn5 KO vs. WT mice (−6.25). Although changes in the mRNA of Cyp27b1 did not reach significance in this gene array, because of the importance of this protein for vitamin D_3 metabolism we measured the protein level. The protein level of Cyp27b1 was highly elevated in KO vs. WT cortex, and as a control it was shown that injected 1α,25-dihydroxyvitamin D_3 lowered the protein in the cortex of both WT and KO mice, as expected (Fig. 2). Also of note is the fact that the mRNA of the group-specific component (Gc) globulin, or DBP, is downregulated in Clcn5 KO kidney proximal tubules (−5). The function of DBP is to carry 25-hydroxyvitamin D_3 from the liver to the bloodstream and then to the proximal tubule, where it is internalized by megalin to release 25-hydroxyvitamin D_3 to the 25-hydroxyvitamin D_3 1α-hydroxylase, Cyp27b1, found there. We wondered how the renal loss of DBP could be compatible with elevated 1α,25-dihydroxyvitamin D_3 in the Clcn5 KO mouse. Thus we measured the level of DBP in blood. DBP was found in the ClCn5 KO but not WT urine, as expected. In the same animals there were equal amounts of DBP in the serum of WT and ClCn5 KO mice (Fig. 3). Similar levels of DBP in the serum of both WT and ClCn5 KO mice suggest that liver synthesis of DBP in the ClCn5 KO keeps pace with losses in the urine.

In the GOMiner summary of the genes for molecular function (Table 2) those for *1*) catalytic activity (172/2,367), *2*) transporter activity (54/553), *3*) oxidoreductase activity (35/396), *4*) hydrolase activity (acting on ester bonds) (25/281), *5*) ion transporter activity (24/263), *6*) iron ion binding (14/138), and *7*) channel or pore class transporter activity (13/125) had the greatest number of changed transcript levels. Other categories with no significant changes in molecular function were signal transducer activity, ion binding, receptor activity, metal ion binding, and actin binding.

In the GOMiner molecular function summary the category with the greatest change is catalytic activity (172/2,367). The genes changed in this category are shown in Table 3. Genes in this catalytic activity category that had the largest mRNA increases in Clcn5 KO/WT proximal tubules included the adenylate cyclase-associated protein Cap1 (9.0). Nevertheless, the Cap1 protein level was not different in the proximal tubules of Clcn5 KO vs. WT mice (Fig. 4). Also included were neuronal PAS domain protein 2 (Npas2) (5.9) and the 5′-nucleotidase gene Nt5e (5.0). Nt5e is found in the brush border of the proximal tubule (11) and is involved in regulation of tubuloglomerular feedback (20). The next highest gene is abhydrolase domain containing 1 (Abhd1) (4.3), a gene of unknown specific function that contains a catalytic domain found in many enzymes. Also of interest is Abca3 (−1.45),

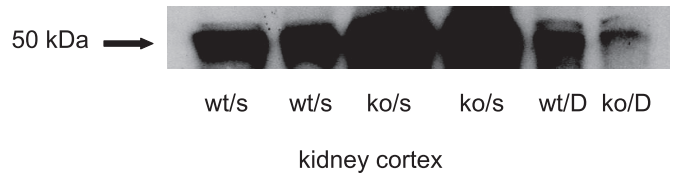

Fig. 2. Western blot of Cyp27b1, the 25-hydroxyvitamin D_3 1α-hydroxylase, in saline-injected (s) or 1α,25-dihydroxyvitamin D_3-injected (D) mice. A total of 20 μg of homogenate was loaded to each lane. The primary antibody was used at 1/400 and the secondary at 1/5,000. The saline-injected Clcn5 KO mice had much more renal Cyp27b1 than the WT mice. Cyp27b1 showed an expected decrease in both WT and KO kidney cortex after injection of 1α,25-dihydroxyvitamin D_3. Representative of 3 studies.

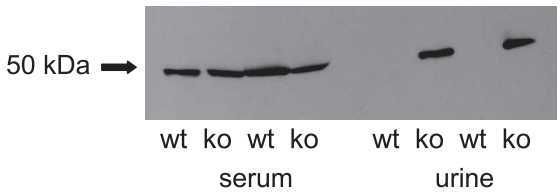

Fig. 3. Western blot of the vitamin D binding protein (DBP) in serum of WT and ClCn5 KO mice. A total of 20 μg of protein was added to each lane. The primary antibody was applied at a dilution of 1/1,000 and the secondary antibody at 1/5,000. DBP was measured in urine and serum of WT and KO mice. Only urine samples showed differences in DBP as previously shown. There was no difference in DBP levels in serum when WT and KO mice were compared. Representative of 2 studies.

which is localized to proximal tubule apical membranes and whose decreased protein expression is associated with renal injury (21). Cytochrome *P*-450 Cyp4a14, an enzyme involved in fatty acid and eicosanoid metabolism, decreased in mRNA by 33-fold in Clcn5 KO. Cyp4a14 is a family of enzymes thought to be very important in lipid homeostasis and signaling.

Over 30 genes in the catalytic activity category are involved in metabolism. Some of these include hydroxysteroid dehydrogenase/reductase (SDR family) member 8 (Dhrs8) (1.62), betaine-homocysteine methyltransferase (Bhmt) (1.6), α-methylacyl-CoA racemase (Amacr) (1.6), fucosyltransferase 9α (1.3), lipoprotein lipase Lpl (−1.5), carnitine palmitoyltransferase 2 (Cpt2) (−1.43), argininosuccinate synthetase 1 (Ass1) (−1.79), methylcrotonoyl-coenzyme A carboxylase 1 (α) (Mccc1) (−1.64), glycine dehydrogenase (Gldc) (−1.73), fucosyltransferase Fut9 (−1.75), and monoglyceride lipase (Mgll) (−1.96, −2.38, −1.67). Many genes in the catalytic activity category are associated with signaling. These genes include guanylate binding protein 1 interferon-inducible (Gbp1) (2.5), protein tyrosine phosphatase, nonreceptor type 8 (Ptpn8) (2.1), phosphodiesterase A1 (calmodulin-dependent) (Pde1a) (2.0), guanine nucleotide binding protein (G protein), β polypeptide 1 (Gnb1) (1.7), calcium/calmodulin-dependent protein kinase I (Camk1) (−1.39), p21 (CDKN1A)-activated kinase 2 (Pak2) (−1.43), guanylate cyclase 1 soluble α3 (Gucy1a3) (−1.56, −2.22), phosphatidylinositol-4-phosphate 5-kinase, type II, β (Pip5k2b) (−1.54), protein kinase, cAMP-dependent, regulatory, type II, α (Prkar2a) (−1.56), protein tyrosine phosphatase, receptor type, F polypeptide (Ptprf) (−1.64), and phosphoinositide 3-kinase, class 2, α polypeptide (Pik3c2a) (−2.0, −1.82).

The second major significantly changed group in the molecular function summary is transporter activity (54/553). The changed genes in this category are Nup210, Vldlr, Slc34a3, Slc10a2, Apoc3, Atox1, Lpl, Dbp, Mcoln1, Mtac2d1, Slcoca1, Atp6v1e, Aqp6, Slc39a8, Aqp3, Garb3, Gc, Slc38a3, Kcne1, Hdlbp, Atp10d, Slc25a20, Syt1, Slc27a1, Prkar2a, Cox6a2, Snap29, Scl7a7, Abcb10, Slc7a13, Maoa, Kdelr2, Cp, Tm9sf2, Slc4a1, Moat6, Slc18a1, Hbb-b1, Rhbg, Atp4a, Clcn3, Abcd4, Slc2a4, Ttr, Slc6a13, Loc208169, Slc8a1, Gjb1, Clcn5, Kcnk5, Pln, Slc30a7, Slc27a7, F5. Of note is the vacuolar H^+-ATPase Atp6v1e1 (1.40), which is involved in acidification of endosomes and lysosomes, a physiological function that is known to be decreased in Dent disease (16, 18), and two potassium channels, Kcne1 (1.43) and Kcnk5 (1.39), that are involved in plasma membrane K transport and perhaps transepithelial transport. Also important are the group of Slc transporters that have significant changes in mRNA that have not been previously been reported.

A list of all significant genes changed (10% FDR) in the proximal tubule gene array is provided in Supplemental Table S2. This table shows, in order, the genes of highest and lowest individual changes rather than the significant groupings of genes as shown in Tables 1 and 2. All other results are available in the NCBI GEO database as series GSE10162 at the link **http://www.ncbi.nlm.nih.gov/geo/query/acc.cgi?token=phwtxcisimisetq&acc=GSE10162**.

DISCUSSION

The results of this array give the fingerprint of changes in the genes from Clcn5 KO compared with WT proximal tubules. The pattern of gene changes is very distinct and can be used in the future for comparison with other renal dysfunction genes affecting endocytosis or acidification of early endosomes. In particular, it might be informative to compare the genes changed in a Fanconi syndrome phenotype or those of Lowe syndrome (26). This disease has the same renal phenotype as Dent disease described here. In Lowe syndrome, a mutation of phosphatidylinositol 4,5-bisphosphate [PtdIns(4,5)P_2] 5-phosphatase causes accumulation of PtdIns(4,5)P_2. This phosphatase is known to be involved in clathrin-mediated endocytosis (9), and mutations of this gene also cause loss of low-molecular-weight proteins.

One of the most unexpected aspects of this work are the changes in lipid metabolism, as judged by the fact that this category has such a large number of genes that were altered in expression when comparing the Clcn5 KO mice proximal tubules and the WT proximal tubules. There is a decrease in mRNA of all of the changed genes in this fatty acid metabolism group. Likewise, the mRNA of Cyp4a14, an enzyme involved in fatty acid and eicosanoid metabolism, is greatly decreased. These changes in metabolism have not been reported previously.

In cholesterol metabolism the most important transcript increase is that of squalene monooxygenase, which is a key regulatory enzyme in cholesterol synthesis. Soluble Hmgcs1 mRNA is upregulated almost twofold, and the cholesterol efflux pump mRNA for Abca1 is decreased. The large increase in mRNA for the ATP citrate lyase gene, which makes acetyl-CoA, is also important in possibly contributing to cholesterologenesis. It has been reported that when the synthesis of cholesterol is inhibited in the endosome for >2 h, the localization patterns of the late endosomes and lysosomes are altered and their mobility is retarded (40). If there are changed amounts of cholesterol present in proximal tubule cells of the Clcn5 KO mice, it is also a possibility that the endosomal pattern is changed and there might be changes in endocytosis as a result. This could not be hypothesized from previous data on Dent disease patients or mice. These data suggest not only that the loss of Clcn5 disrupts the endosomal pathway but that other secondary factors could also affect endocytosis. For example, caveolin 2 mRNA is also upregulated. Caveolin 2-mediated transport is a process that is cholesterol dependent. Upregulation of caveolin protein could affect caveolin/cholesterol-mediated endocytosis. To date, the process of caveolin-mediated endocytosis has not been evaluated in the Clcn5 KO. Could other compensatory pathways of endocytosis be upregu-

Table 2. *Gene Ontology: molecular function*

GO ID	Total	Changed	*P* Value	Term
3824	2367	172	0.0037	Catalytic activity
5215	553	54	0.0004	Transporter activity
16491	396	35	0.0192	Oxidoreductase activity
16788	281	25	0.041	Hydrolase activity, acting on ester bonds
15075	263	24	0.0347	Ion transporter activity
5506	138	14	0.0454	Iron ion binding
15267	125	13	0.0446	Channel or pore class transporter activity
16789	47	11	0.0001	Carboxylic ester hydrolase activity
16705	59	11	0.0008	Oxidoreductase activity
4497	52	10	0.0011	Monooxygenase activity
46983	71	10	0.0114	Protein dimerization activity
16746	79	10	0.023	Transferase activity, transferring acyl groups
20037	54	9	0.0054	Heme binding
46906	54	9	0.0054	Tetrapyrrole binding
5516	54	8	0.017	Calmodulin binding
4857	63	8	0.0391	Enzyme inhibitor activity
4759	17	7	<0.0001	Serine esterase activity
4091	17	7	<0.0001	Carboxylesterase activity
8238	37	7	0.0067	Exopeptidase activity
19842	40	7	0.0104	vitamin binding
4252	52	7	0.0396	Serine-type endopeptidase activity
8236	54	7	0.0472	Serine-type peptidase activity
5539	33	6	0.0144	Glycosaminoglycan binding
1871	35	6	0.019	Pattern binding
30247	35	6	0.019	Polysaccharide binding
15645	8	5	<0.0001	Fatty acid ligase activity
16877	13	5	0.0008	Ligase activity, forming carbon-sulfur bonds
5496	23	5	0.0118	Steroid binding
5319	24	5	0.0141	Lipid transporter activity
5507	26	5	0.0198	Copper ion binding
8201	27	5	0.0231	Heparin binding
16289	6	4	0.0002	CoA hydrolase activity
4467	7	4	0.0004	Long-chain fatty acid-CoA ligase activity
5520	15	4	0.0114	Insulin-like growth factor binding
8483	16	4	0.0145	Transaminase activity
16712	17	4	0.018	Oxidoreductase activity
4177	19	4	0.0267	Aminopeptidase activity
16769	21	4	0.0374	Transferase activity, transferring nitrogenous groups
5279	22	4	0.0435	Amino acid-polyamine transporter activity
3823	22	4	0.0435	Antigen binding
15203	22	4	0.0435	Polyamine transporter activity
5499	4	3	0.0009	Vitamin D binding
16291	4	3	0.0009	Acyl-CoA thioesterase activity
16290	5	3	0.0021	Palmitoyl-CoA hydrolase activity
16638	7	3	0.0068	Oxidoreductase activity, CH-NH_2 donors
1664	11	3	0.0267	G protein-coupled receptor binding
42379	11	3	0.0267	Chemokine receptor binding
8009	11	3	0.0267	Chemokine activity
19239	12	3	0.034	Deaminase activity
16814	12	3	0.034	Hydrolase activity, in cyclic amidines
16628	12	3	0.034	Oxidoreductase activity, NAD or NADP as acceptor
50381	12	3	0.034	Unspecific monooxygenase activity
15297	13	3	0.0423	Antiporter activity
18685	2	2	0.0038	Alkane 1-monooxygenase activity
16715	2	2	0.0038	Oxidoreductase activity, reduced ascorbate as one donor
16713	2	2	0.0038	Oxidoreductase activity, reduced iron-sulfur protein
4421	2	2	0.0038	Hydroxymethylglutaryl-CoA synthase activity
8670	2	2	0.0038	2,4-Dienoyl-CoA reductase (NADPH) activity
3988	3	2	0.011	Acetyl-CoA C-acyltransferase activity
42605	3	2	0.011	Peptide antigen binding
46912	4	2	0.0211	Transferase activity, transferring acyl groups, acyl groups
45012	5	2	0.0337	MHC class II receptor activity
16840	5	2	0.0337	Carbon-nitrogen lyase activity
51183	5	2	0.0337	Vitamin transporter activity
4383	5	2	0.0337	Guanylate cyclase activity
15174	5	2	0.0337	Basic amino acid transporter activity
16641	6	2	0.0485	Oxidoreductase activity, oxygen as acceptor
4372	6	2	0.0485	Glycine hydroxymethyltransferase activity

Table 3. *Gene Ontology group 3824, catalytic activity*

Gene Symbol	Change	Description
		Upregulated in Clcn5 KO
CAP1	8.97	Adenylate cyclase-associated protein 1 (yeast)
NPAS2	5.94	Neuronal PAS domain protein 2
NSD1	5.00	Nuclear receptor-binding SET-domain protein 1
ABHD1	4.30	Abhydrolase domain containing 1
UGT2B5	4.21	UDP-glucuronosyltransferase 2 family, member 5
NT5E	4.20	5′-Nucleotidase, ecto
MEP1B	2.65	Meprin 1β
ATP10D	2.56	ATPase, Class V, type 10D
GBP1	2.52	Guanylate nucleotide binding protein 1
PIM1	2.39	Proviral integration site 1
POLI	2.29	Polymerase (DNA directed), ι
PROZ	2.26	Protein Z, vitamin K-dependent plasma glycoprotein
ATP4A	2.23	ATPase, H^+/K^+ transporting, α polypeptide
FTCD	2.11	Formiminotransferase cyclodeaminase
PTPN8	2.10	Protein tyrosine phosphatase, nonreceptor type 8
MCM6	2.08	Minichromosome maintenance deficient 6 (*S. cerevisiae*)
SQLE	2.07	Squalene epoxidase
PFKFB3	2.02	6-Phosphofructo-2-kinase/fructose-2,6-biphosphatase 3
KAT2	1.99	Kynurenine aminotransferase II
PDE1A	1.95	Phosphodiesterase 1A, calmodulin-dependent
HMGCS1	1.94	3-Hydroxy-3-methylglutaryl-coenzyme A synthase 1
STK25	1.84	Serine/threonine kinase 25 (yeast)
SOX4	1.80	Suppressor of cytokine signaling 4
BDH	1.79	3-Hydroxybutyrate dehydrogenase (heart, mitochondrial)
ACP6	1.78	Acid phosphatase 6, lysophosphatidic
EPM2A	1.75	Epilepsy, progressive myoclonic epilepsy, type 2 gene α
DAPK1	1.71	Death-associated protein kinase 1
GNB1	1.68	Guanine nucleotide binding protein, β1
HAO3	1.68	Hydroxyacid oxidase (glycolate oxidase) 3
SHMT1	1.68	Serine hydroxymethyl transferase 1 (soluble)
RRAS2	1.64	Related RAS viral (r-ras) oncogene homolog 2
A530088I07RIK	1.62	Cysteine-type endopeptidase activity
DHRS8	1.62	Dehydrogenase/reductase (SDR family) member 8
TOP2B	1.62	Topoisomerase (DNA) IIβ
4732435N03RIK	1.60	β1,4 *N*-acetylgalactosaminyltransferase
BHMT	1.60	Betaine-homocysteine methyltransferase
G6PDX	1.60	Glucose-6-phosphate dehydrogenase X-linked
AMACR	1.59	α-Methylacyl-CoA racemase
GNB4	1.59	Guanine nucleotide binding protein, β4
CHM	1.58	Choroidermia
UAP1	1.58	UDP-*N*-acetylglucosamine pyrophosphorylase 1
CDKL1	1.57	Cyclin-dependent kinase-like 1 (CDC2-related kinase)
CN1	1.57	Carnosinase 1
PAX8	1.57	Paired box gene 8
SH3KBP1	1.57	SH3-domain kinase binding protein 1
4631424J17RIK	1.55	PWWP domain containing 2A
IGF1R	1.55	Insulin-like growth factor I receptor
LATS1	1.55	Large tumor suppressor
PTER	1.54	Phosphotriesterase related
Pyroxd1	1.53	Pyridine nucleotide-disulfide oxidoreductase domain 1
ENPEP	1.52	Glutamyl aminopeptidase
1700037C18RIK	1.51	Hypothetical protein LOC73261
PIGA	1.50	Phosphatidylinositol glycan, class A
COX6A2	1.48	Cytochrome-*c* oxidase, subunit VI a, polypeptide 2
TNFAIP3	1.48	Tumor necrosis factor, α-induced protein 3
TRIO	1.48	Triple functional domain (PTPRF interacting)
ADAMTS15	1.46	Disintegrin-like metalloprotease with thrombospondin type 1 motif, 15
PPT1	1.46	Palmitoyl-protein thioesterase 1
ADAMTS1	1.45	Disintegrin-like metalloprotease with thrombospondin type 1 motif, 1
BRD4	1.45	Bromodomain containing 4
LIP1	1.45	Lipin 1
CP	1.44	Ceruloplasmin
3110056O03RIK	1.44	Signal peptide peptidase-like 2B
ECGF1	1.43	Endothelial cell growth factor 1 (platelet-derived)
ATP6V1E1	1.40	ATPase, H^+ transporting, V1 subunit E isoform 1
CHST7	1.39	Carbohydrate (*N*-acetylglucosamino) sulfotransferase 7
SMT3H1	1.39	SMT3 (suppressor of mif two, 3) homolog 1 (*S. cerevisiae*)

Continued

Table 3.—*Continued*

Gene Symbol	Change	Description
NEO1	1.37	Neogenin
TYROBP	1.37	TYRO protein tyrosine kinase binding protein
NCOA1	1.35	Nuclear receptor coactivator 1
THEA	1.35	Thioesterase, adipose associated
ALDH2	1.34	Aldehyde dehydrogenase 2, mitochondrial
ACE2	1.31	Angiotensin I-converting enzyme (peptidyl-dipeptidase A) 2
		Downregulated in Clcn5 KO
CASK	−1.30	Calcium/calmodulin-dependent serine protein kinase
MAPK14	−1.30	Mitogen-activated protein kinase 14
AADAC	−1.35	Arylacetamide deacetylase (esterase)
ACAA1	−1.35	Acetyl-coenzyme A acyltransferase 1A
BUCS1	−1.35	Butyryl coenzyme A synthetase 1
C2	−1.37	Complement component 2 (within H-2S)
HSD3B4	−1.37	Hydroxysteroid dehydrogenase-4, δ <5>-3-β
CAMK1	−1.39	Calcium/calmodulin-dependent protein kinase I
DPP7	−1.39	Dipeptidylpeptidase 7
GALNS	−1.41	Galactosamine (*N*-acetyl)-6-sulfate sulfatase
TYMS	−1.41	Thymidylate synthase
CYP2D26	−1.43	Cytochrome *P*-450, family 2, subfamily d, polypeptide 26
DCI	−1.43	Dodecenoyl-coenzyme A δ isomerase
DECR2	−1.43	2,4-Dienoyl-coenzyme A reductase 2, peroxisomal
GUCY1B3	−1.43	Guanylate cyclase 1, soluble, β3
ABCA3	−1.45	ATP-binding cassette, subfamily A (ABC1), member 3
CPT2	−1.45	Carnitine palmitoyltransferase 2
NPL	−1.45	*N*-acetylneuraminate pyruvate lyase
PAK2	−1.45	p21 (CDKN1A)-activated kinase 2
SDFR2	−1.45	Stromal cell-derived factor receptor 2
AMPD3	−1.47	AMP deaminase 3
APRT	−1.47	Adenine phosphoribosyl transferase
COL4A3BP	−1.47	Collagen, type IV, α3 (Goodpasture antigen) binding protein
DECR1	−1.47	2,4-Dienoyl CoA reductase 1, mitochondrial
HSD11B1	−1.47	Hydroxysteroid 11-β dehydrogenase 1
ACAA2	−1.49	Acetyl-coenzyme A acyltransferase 2
B3GALT3	−1.49	UDP-Gal:βGlcNAc β1,3-galactosyltransferase, polypeptide 3
CYP2D9	−1.49	Cytochrome *P*-450, family 2, subfamily d, polypeptide 9
ENPP2	−1.49	Ectonucleotide pyrophosphatase/phosphodiesterase 2
LPL	−1.49	Lipoprotein lipase
SH3GL2	−1.49	SH3-domain GRB2-like 2
SRD5A2	−1.49	Steroid 5 α-reductase 2
ABCA1	−1.52	Cholesterol efflux transporter
PPICAP	−1.52	Peptidylprolyl isomerase C-associated protein
DPP4	−1.54	Dipeptidylpeptidase 4
MAOA	−1.54	Monoamine oxidase A
PIP5K2B	−1.54	Phosphatidylinositol-4-phosphate 5-kinase, type II, β
TBXAS1	−1.54	Thromboxane A synthase 1, platelet
3222402P14RIK	−1.54	α-Isoform of regulatory subunit B″, protein phosphatase 2
2210023G05RIK	−1.56	Hypothetical protein LOC72361
FACL4	−1.56	Fatty acid-coenzyme A ligase, long chain 4
NUDT7	−1.56	Nudix (nucleoside diphosphate linked moiety X)-type motif 7
PRKAR2A	−1.56	Protein kinase, cAMP dependent regulatory, type IIα
ABCB10	−1.59	ATP-binding cassette, subfamily B (MDR/TAP), member 10
CYP2A4	−1.59	Cytochrome *P*-450, family 2, subfamily a, polypeptide 4
GDA	−1.61	Guanine deaminase
MGST1	−1.61	Microsomal glutathione *S*-transferase 1
FBXL10	−1.64	F-box and leucine-rich repeat protein 10
MCCC1	−1.64	Methylcrotonoyl-coenzyme A carboxylase 1 (α)
PTPRF	−1.64	Protein tyrosine phosphatase, receptor type, F
FACL3	−1.67	Fatty acid coenzyme A ligase, long chain 3
GLO1	−1.67	glyoxalase 1
SLC27A1	−1.67	Solute carrier family 27 (fatty acid transporter), member 1
SIAT7B	−1.69	Sialyltransferase 7B
GLDC	−1.72	Glycine decarboxylase
PLD1	−1.72	Phospholipase D1
CML2	−1.75	Camello-like 2
FUT9	−1.75	Fucosyltransferase 9
GALC	−1.75	Galactosylceramidase
ASS1	−1.79	Argininosuccinate synthetase 1

Continued

Table 3.—*Continued*

Gene Symbol	Change	Description
ABCD4	−1.82	ATP-binding cassette, subfamily D (ALD), member 4
GUCY1A3	−1.82	Guanylate cyclase 1, soluble, α3
POLD4	−1.85	Polymerase (DNA-directed), δ4
PMSCL1	−1.89	Polymyositis/scleroderma autoantigen 1
FACL2	−1.92	Fatty acid coenzyme A ligase, long chain 2
HPGD	−1.92	Hydroxyprostaglandin dehydrogenase 15 (NAD)
KLK16	−1.92	Kallikrein 16
PIK3C2A	−1.92	Phosphatidylinositol 3-kinase, α polypeptide
ASNS	−2.00	Asparagine synthetase
PAM	−2.00	Peptidylglycine α-amidating monooxygenase
PTE2A	−2.00	Peroxisomal acyl-CoA thioesterase 2A
TGM1	−2.00	Transglutaminase 1, K polypeptide
MTHFD2	−2.08	Methylenetetrahydrofolate dehydrogenase
RENT1	−2.08	Regulator of nonsense transcripts 1
Pm20d1	−2.17	Peptidase M20 domain containing 1
HEXA	−2.17	Hexosaminidase A
MGLL	−2.22	Monoglyceride lipase
PSAT1	−2.22	Phosphoserine aminotransferase 1
Tmem195	−2.27	Transmembrane protein 195
CTE1	−2.27	Cytosolic acyl-CoA thioesterase 1
HMOX1	−2.27	Heme oxygenase (decycling) 1
BCDO2	−2.33	β-Carotene 9′,10′-dioxygenase 2
CPE	−2.33	Carboxypeptidase E
MTE1	−2.33	Mitochondrial acyl-CoA thioesterase 1
CML3	−2.38	Camello-like 3
PRDX2	−2.38	Peroxiredoxin 2
PDK4	−2.50	Pyruvate dehydrogenase kinase, isoenzyme 4
VNN1	−2.63	Vanin 1
BLVRB	−2.78	Biliverdin reductase B [flavin reductase (NADPH)]
SUPT16H	−2.94	Suppressor of Ty 16 homolog (*S. cerevisiae*)
CES1	−3.03	Carboxylesterase 1
AGXT2L1	−3.57	Alanine-glyoxylate aminotransferase 2-like 1
CYP4A10	−3.57	Cytochrome *P*-450, family 4, subfamily a, polypeptide 10
CAR3	−4.00	Carbonic anhydrase 3
F5	−4.55	Coagulation factor V
HMGCS2	−4.55	3-Hydroxy-3-methylglutaryl-coenzyme A synthase 2
CYP24A1	−5.56	Cytochrome *P*-450, family 24, subfamily a, polypeptide 1
PHGDH	−16.67	3-Phosphoglycerate dehydrogenase
CYP4A14	−33.33	Cytochrome *P*-450, family 4, subfamily a, polypeptide 14

lated in response to the decrease in receptor-mediated endocytosis caused by the loss of Clcn5?

Surprisingly, there are not many mRNA changes in pathways that are likely to be involved in protein reabsorption in the proximal tubule. It was previously shown that megalin protein is decreased in the Clcn5 KO mouse (10), but there is no change in the mRNA shown in this gene array. Likewise, there is no change in the mRNA of the Slc34a1 (Npt2a) transporter, even though this protein is decreased in the Clcn5 KO mouse kidney cortex compared with WT (34). Two transporters do show reductions in mRNA that could correspond to the physiological phenotype of Dent disease. If decreases in Nhe10/sperm and the phosphate transporter Slc34a3 mRNA translate into changes in transporter protein, they may contribute to the decreased uptake of both sodium and phosphate in the proximal tubules. The decrease in Nhe10/sperm mRNA is found at the protein level, and this protein has been found to localize at the plasma membrane (44). The presence of NHE10/sperm in kidney proximal tubule has not been reported previously. It is possible that decreases in these transporters contribute to the changes already found for Slc9a3 (Nhe3) and Slc34a1 (Npt2a). Both Nhe3 and Npt2a are mislocalized away from the plasma membrane in Clcn5 KO mouse proximal tubules. It is thought that this is the cause of the phosphaturia and polyuria in the Clcn5 KO and in Dent disease patients.

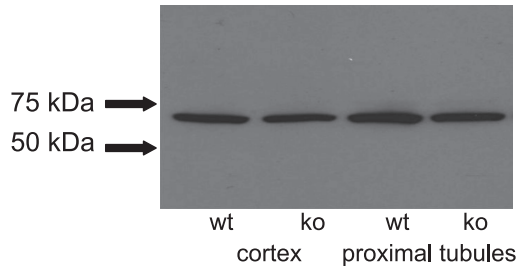

Fig. 4. Western blot of the adenylate cyclase-associated protein Cap1. A total of 20 μg of proximal tubule or kidney cortex was added to each lane. The primary antibody was used at 1/2,000 and the secondary antibody at 1/5,000. The mRNA of Cap1 is increased 5- to 9-fold as indicated by the present gene array, yet protein levels are nearly identical, suggesting regulation at the translational level. Representative of 3 studies.

Another transporter with increased mRNA expression that may have physiological relevance to the Dent phenotype is Clc3, which is in the same class of intracellular ion chloride proton exchangers as Clc5. Clc3 is thought to be an intracellular exchanger, but its exact location in the proximal tubule

cell is still unknown. It has been hypothesized that Clc3 or 4 and Clc5 may heterodimerize (31). If this is so, and if the protein also increases as the mRNA does, one would expect that an increase in the ion channel protein might mitigate the symptoms of Dent disease such as low-molecular-weight proteinuria. But this would only occur if the Clc3 ion channels segregated to the same vesicle population as Clcn5 and if there was enough Clc3 protein to take over the function of Clcn5. The idea that Clc3 may participate in the uptake of low-molecular-weight proteins has not been verified. This warrants further investigation with the Clcn3 KO mouse to determine whether loss of Clc3 in proximal tubules causes loss of low-molecular-weight proteins. Cystic fibrosis transmembrane conductance regulator (Cftr) knockout mice and cystic fibrosis patients with the ΔF508 CFTR deletion have a mild low-molecular-weight proteinuria and decreased amounts of megalin in the kidney cortex (22). This suggests that CFTR may also function like Clc5 to acidify a population of vesicles that are involved in megalin-mediated low-molecular-weight protein uptake. A gene array of the renal proximal tubules from the Cftr knockout mouse may be informative and give some similar changes in transport genes as Clcn5.

Several genes involved in vesicle-mediated transport or vesicle turnover are changed. The stabilin-2 gene is decreased. Stabilins are situated in the early endosome. The change in this gene could signal another faulty process underlying decreased receptor-mediated endocytosis in the Clcn5 KO mouse proximal tubule. In vesicle-mediated transport one of the most interesting changes in mRNA is that of the Cap1 gene. It has been reported that Clc5 binds cofilin (19); if Clc5 also binds profilin, then interaction with the Cap1 protein may also have relevance to movement through the actin matrix. Snap29 mRNA is down in Clcn5 KO tubules (−1.32). Snap29 protein is known to act as a negative modulator of neurotransmitter release, probably by slowing fusion events and vesicle turnover. Snap23, not changed in the Clcn5 KO tissue, regulates plasma membrane vesicle fusion events. Snap23 is downregulated at the mRNA level in mouse lung cystic fibrosis tissue (48). The mutated gene product of cystic fibrosis (CFTR) is a chloride channel that has decreased stability on the plasma membrane (27).

The calcium/vitamin D_3 axis, including phosphate transport, is altered in Dent disease patients. Dent disease patients have elevated 1α,25-dihydroxyvitamin D_3, normal to low PTH, and renal loss of calcium and phosphate. These outcomes have also received attention in the Clcn5 KO mouse models. In this gene array we found that the 1α,25-dihydroxyvitamin D_3 24-hydroxylase (Cyp24a1) is downregulated significantly in proximal tubules of Clcn5 KO mice compared with WT mice, which is consistent with elevated levels of the active hormone 1α,25-dihydroxyvitamin D_3 in the Guggino mouse model. The gene array performed by Maritzen et al. (29) showed an increase in the mRNA for the 25-hydroxyvitamin D_3 1α-hydroxylase (Cyp27b1) in the Clcn5 KO mouse kidney. Although this present gene array did not show significant changes in the 25-hydroxyvitamin D_3 1α-hydroxylase (Cyp27b1) mRNA, we investigated the protein levels of the gene product. In protein assays for Cyp27b1 there was a significant increase in the amount of Cyp27b1 in the Clcn5 KO mouse cortex compared with WT cortex. These results suggest that the significant increase in Cyp27b1 may be the cause of the increased concentration of 1α,25-dihydroxyvitamin D_3 in the Guggino Clcn5 KO mouse and perhaps in Dent disease patients. Although 25-hydroxyvitamin D_3 levels are normal in this mouse, the enzyme may still be substrate limited because of decreased uptake of DBP via megalin into the proximal tubules. Although DBP is lost in the urine of the Clcn5 KO mouse, serum levels of DBP are the same in WT and Clcn5 KO mice. Thus filtered DBP is not rate limiting to 24-hydroxyvitamin D_3 uptake in the proximal tubule. When comparing this proximal tubule gene array to that of the Jentsch whole kidney gene array, there is overlap of only two genes, namely, Cyp24a1 and Slc10a2. Interestingly, Maritzen et al. found that Slc10a2 mRNA was downregulated, which corresponds to lowered levels of 1α,25-dihydroxyvitamin D_3 in the Jentsch Clcn5 KO mice. It is possible that the great number of genes up- or downregulated in the Guggino gene array is a result of the pleiotropic effects caused by elevated serum 1α,25-dihydroxyvitamin D_3. A gene array done on whole kidney of 1α,25-dihydroxyvitamin D_3-treated wild-type mice compared with untreated wild-type mice shows that 94 genes were up- or downregulated (24). The vitamin D_3 hydroxylases were changed, but no other changed genes were common to those in the Clcn5 gene arrays. Most importantly, the many genes associated with lipid metabolism, transport, or vesicular endocytosis are not changed in the 1α,25-dihydroxyvitamin D_3 injection model.

In summary, we have shown that there are numerous changes in gene transcript levels in the comparison of proximal tubules of WT and Clcn5 KO mice. This gene array gives the fingerprint of mRNA compensations that occur with the loss of Clc5 in the proximal tubules of this mouse. These data may be compared with other gene arrays to determine what classes of genes change in a particular phenotype. Outcomes, in terms of functional or protein changes for these gene transcript changes, await further study.

GRANTS

We acknowledge funding from National Institute of Diabetes and Digestive and Kidney Diseases Grants DK-032753 to W. B. Guggino and DK-072084 to S. E. Guggino.

REFERENCES

1. **Alexandrov K, Horiuchi H, Steele-Mortimer O, Seabra MC, Zerial M.** Rab escort protein-1 is a multifunctional protein that accompanies newly prenylated rab proteins to their target membranes. *EMBO J* 13: 5262–5273, 1994.
2. **Anderson RG.** Caveolae: where incoming and outgoing messengers meet. *Proc Natl Acad Sci USA* 90: 10909–10913, 1993.
3. **Ashburner M, Ball CA, Blake JA, Botstein D, Butler H, Cherry JM, Davis AP, Dolinski K, Dwight SS, Eppig JT, Harris MA, Hill DP, Issel-Tarver L, Kasarskis A, Lewis S, Matese JC, Richardson JE, Ringwald M, Rubin GM, Sherlock G.** Gene ontology: tool for the unification of biology. The Gene Ontology Consortium. *Nat Genet* 25: 25–29, 2000.
4. **Benjamini Y, Hochberg Y.** Controlling the false discovery rate: a practical and powerful approach to multiple testing. *J R Stat Soc B* 57: 289–300, 1995.
5. **Bertling E, Hotulainen P, Mattila PK, Matilainen T, Salminen M, Lappalainen P.** Cyclase-associated protein 1 (CAP1) promotes cofilin-induced actin dynamics in mammalian nonmuscle cells. *Mol Biol Cell* 15: 2324–2334, 2004.
6. **Bertling E, Quintero-Monzon O, Mattila PK, Goode BL, Lappalainen P.** Mechanism and biological role of profilin-Srv2/CAP interaction. *J Cell Sci* 120: 1225–1234, 2007.
7. **Cebotaru V, Kaul S, Devuyst O, Cai H, Racusen L, Guggino WB, Guggino SE.** High citrate diet delays progression of renal insufficiency in

the ClC-5 knockout mouse model of Dent's disease. *Kidney Int* 68: 642–652, 2005.
8. **Chen X, Chen F, Liu S, Glaeser H, Dawson PA, Hofmann AF, Kim RB, Shneider BL, Pang KS.** Transactivation of rat apical sodium-dependent bile acid transporter and increased bile acid transport by 1α,25-dihydroxyvitamin D_3 via the vitamin D receptor. *Mol Pharmacol* 69: 1913–1923, 2006.
9. **Choudhury R, Diao A, Zhang F, Eisenberg E, Saint-Pol A, Williams C, Konstantakopoulos A, Lucocq J, Johannes L, Rabouille C, Greene LE, Lowe M.** Lowe syndrome protein OCRL1 interacts with clathrin and regulates protein trafficking between endosomes and the trans-Golgi network. *Mol Biol Cell* 16: 3467–3479, 2005.
10. **Christensen EI, Devuyst O, Dom G, Nielsen R, Van der Smissen P, Verroust P, Leruth M, Guggino WB, Courtoy PJ.** Loss of chloride channel ClC-5 impairs endocytosis by defective trafficking of megalin and cubilin in kidney proximal tubules. *Proc Natl Acad Sci USA* 100: 8472–8477, 2003.
11. **Dawson TP, Gandhi R, Le HM, Kaissling B.** Ecto-5′-nucleotidase: localization in rat kidney by light microscopic histochemical and immunohistochemical methods. *J Histochem Cytochem* 37: 39–47, 1989.
12. **Devuyst O, Christie PT, Courtoy PJ, Beauwens R, Thakker RV.** Intra-renal and subcellular distribution of the human chloride channel, CLC-5, reveals a pathophysiological basis for Dent's disease. *Hum Mol Genet* 8: 247–257, 1999.
13. **Fisher SE, van Bakel I, Lloyd SE, Pearce SH, Thakker RV, Craig IW.** Cloning and characterization of CLCN5, the human kidney chloride channel gene implicated in Dent disease (an X-linked hereditary nephrolithiasis). *Genomics* 29: 598–606, 1995.
14. **Guggino SE.** Mechanisms of disease: what can mouse models tell us about the molecular processes underlying Dent disease? *Nat Clin Pract Nephrol* 3: 449–455, 2007.
15. **Gunther W, Luchow A, Cluzeaud F, Vandewalle A, Jentsch TJ.** ClC-5, the chloride channel mutated in Dent's disease, colocalizes with the proton pump in endocytotically active kidney cells. *Proc Natl Acad Sci USA* 95: 8075–8080, 1998.
16. **Gunther W, Piwon N, Jentsch TJ.** The ClC-5 chloride channel knock-out mouse—an animal model for Dent's disease. *Pflügers Arch* 445: 456–462, 2003.
17. **Hansen B, Longati P, Elvevold K, Nedredal GI, Schledzewski K, Olsen R, Falkowski M, Kzhyshkowska J, Carlsson F, Johansson S, Smedsrod B, Goerdt S, Johansson S, McCourt P.** Stabilin-1 and stabilin-2 are both directed into the early endocytic pathway in hepatic sinusoidal endothelium via interactions with clathrin/AP-2, independent of ligand binding. *Exp Cell Res* 303: 160–173, 2005.
18. **Hara-Chikuma M, Wang Y, Guggino SE, Guggino WB, Verkman AS.** Impaired acidification in early endosomes of ClC-5 deficient proximal tubule. *Biochem Biophys Res Commun* 329: 941–946, 2005.
19. **Hryciw DH, Wang Y, Devuyst O, Pollock CA, Poronnik P, Guggino WB.** Cofilin interacts with ClC-5 and regulates albumin uptake in proximal tubule cell lines. *J Biol Chem* 278: 40169–40176, 2003.
20. **Huang DY, Vallon V, Zimmermann H, Koszalka P, Schrader J, Osswald H.** Ecto-5′-nucleotidase (cd73)-dependent and -independent generation of adenosine participates in the mediation of tubuloglomerular feedback in vivo. *Am J Physiol Renal Physiol* 291: F282–F288, 2006.
21. **Huls M, van den Heuvel JJ, Dijkman HB, Russel FG, Masereeuw R.** ABC transporter expression profiling after ischemic reperfusion injury in mouse kidney. *Kidney Int* 69: 2186–2193, 2006.
22. **Jouret F, Bernard A, Hermans C, Dom G, Terryn S, Leal T, Lebecque P, Cassiman JJ, Scholte BJ, de Jonge HR, Courtoy PJ, Devuyst O.** Cystic fibrosis is associated with a defect in apical receptor-mediated endocytosis in mouse and human kidney. *J Am Soc Nephrol* 18: 707–718, 2007.
23. **Leheste JR, Rolinski B, Vorum H, Hilpert J, Nykjaer A, Jacobsen C, Aucouturier P, Moskaug JO, Otto A, Christensen EI, Willnow TE.** Megalin knockout mice as an animal model of low molecular weight proteinuria. *Am J Pathol* 155: 1361–1370, 1999.
24. **Li X, Zheng W, Li YC.** Altered gene expression profile in the kidney of vitamin D receptor knockout mice. *J Cell Biochem* 89: 709–719, 2003.
25. **Lloyd SE, Pearce SH, Fisher SE, Steinmeyer K, Schwappach B, Scheinman SJ, Harding B, Bolino A, Devoto M, Goodyer P, Rigden SP, Wrong O, Jentsch TJ, Craig IW, Thakker RV.** A common molecular basis for three inherited kidney stone diseases. *Nature* 379: 445–449, 1996.
26. **Lowe CU, Terrey M, MacLachlan EA.** Organic-aciduria, decreased renal ammonia production, hydrophthalmos, and mental retardation; a clinical entity. *AMA Am J Dis Child* 83: 164–184, 1952.
27. **Lukacs GL, Chang XB, Bear C, Kartner N, Mohamed A, Riordan JR, Grinstein S.** The delta F508 mutation decreases the stability of cystic fibrosis transmembrane conductance regulator in the plasma membrane. Determination of functional half-lives on transfected cells. *J Biol Chem* 268: 21592–21598, 1993.
28. **Luyckx VA, Goda FO, Mount DB, Nishio T, Hall A, Hebert SC, Hammond TG, Yu AS.** Intrarenal and subcellular localization of rat CLC5. *Am J Physiol Renal Physiol* 275: F761–F769, 1998.
29. **Maritzen T, Rickheit G, Schmitt A, Jentsch TJ.** Kidney-specific up-regulation of vitamin D3 target genes in ClC-5 KO mice. *Kidney Int* 70: 79–87, 2006.
30. **Melia TJ Jr.** Putting the clamps on membrane fusion: how complexin sets the stage for calcium-mediated exocytosis. *FEBS Lett* 581: 2131–2139, 2007.
31. **Mohammad-Panah R, Harrison R, Dhani S, Ackerley C, Huan LJ, Wang Y, Bear CE.** The chloride channel ClC-4 contributes to endosomal acidification and trafficking. *J Biol Chem* 278: 29267–29277, 2003.
32. **Mora R, Bonilha VL, Marmorstein A, Scherer PE, Brown D, Lisanti MP, Rodriguez-Boulan E.** Caveolin-2 localizes to the golgi complex but redistributes to plasma membrane, caveolae, and rafts when co-expressed with caveolin-1. *J Biol Chem* 274: 25708–25717, 1999.
33. **Morita T, Hanaoka K, Morales MM, Montrose-Rafizadeh C, Guggino WB.** Cloning and characterization of maxi K^+ channel α-subunit in rabbit kidney. *Am J Physiol Renal Physiol* 273: F615–F624, 1997.
34. **Piwon N, Gunther W, Schwake M, Bosl MR, Jentsch TJ.** ClC-5 Cl^--channel disruption impairs endocytosis in a mouse model for Dent's disease. *Nature* 408: 369–373, 2000.
35. **Pol A, Martin S, Fernandez MA, Ingelmo-Torres M, Ferguson C, Enrich C, Parton RG.** Cholesterol and fatty acids regulate dynamic caveolin trafficking through the Golgi complex and between the cell surface and lipid bodies. *Mol Biol Cell* 16: 2091–2105, 2005.
36. **Rocke DM, Lorenzato M.** A two-component model for measurement error in analytical chemistry. *Technometrics* 37: 176–184, 1995.
37. **Scheel O, Zdebik AA, Lourdel S, Jentsch TJ.** Voltage-dependent electrogenic chloride/proton exchange by endosomal CLC proteins. *Nature* 436: 424–427, 2005.
38. **Scheinman SJ.** X-linked hypercalciuric nephrolithiasis: clinical syndromes and chloride channel mutations. *Kidney Int* 53: 3–17, 1998.
39. **Silva IV, Cebotaru V, Wang H, Wang XT, Wang SS, Guo G, Devuyst O, Thakker RV, Guggino WB, Guggino SE.** The ClC-5 knockout mouse model of Dent's disease has renal hypercalciuria and increased bone turnover. *J Bone Miner Res* 18: 615–623, 2003.
40. **Sugii S, Lin S, Ohgami N, Ohashi M, Chang CC, Chang TY.** Roles of endogenously synthesized sterols in the endocytic pathway. *J Biol Chem* 281: 23191–23206, 2006.
41. **Terada Y, Moriyama T, Martin BM, Knepper MA, Garcia-Perez A.** RT-PCR microlocalization of mRNA for guanylyl cyclase-coupled ANF receptor in rat kidney. *Am J Physiol Renal Fluid Electrolyte Physiol* 261: F1080–F1087, 1991.
42. **Trommsdorff M, Gotthardt M, Hiesberger T, Shelton J, Stockinger W, Nimpf J, Hammer RE, Richardson JA, Herz J.** Reeler/Disabled-like disruption of neuronal migration in knockout mice lacking the VLDL receptor and ApoE receptor 2. *Cell* 97: 689–701, 1999.
43. **Tusher VG, Tibshirani R, Chu G.** Significance analysis of microarrays applied to the ionizing radiation response. *Proc Natl Acad Sci USA* 98: 5116–5121, 2001.
44. **Wang D, Hu J, Bobulescu IA, Quill TA, McLeroy P, Moe OW, Garbers DL.** A sperm-specific Na^+/H^+ exchanger (sNHE) is critical for expression and in vivo bicarbonate regulation of the soluble adenylyl cyclase (sAC). *Proc Natl Acad Sci USA* 104: 9325–9330, 2007.
45. **Wang D, King SM, Quill TA, Doolittle LK, Garbers DL.** A new sperm-specific Na^+/H^+ exchanger required for sperm motility and fertility. *Nat Cell Biol* 5: 1117–1122, 2003.
46. **Wang SS, Devuyst O, Courtoy PJ, Wang XT, Wang H, Wang Y, Thakker RV, Guggino S, Guggino WB.** Mice lacking renal chloride channel, CLC-5, are a model for Dent's disease, a nephrolithiasis disorder associated with defective receptor-mediated endocytosis. *Hum Mol Genet* 9: 2937–2945, 2000.

47. **Wang XT, Nagaba Y, Cross HS, Wrba F, Zhang L, Guggino SE.** The mRNA of L-type calcium channel elevated in colon cancer: protein distribution in normal and cancerous colon. *Am J Pathol* 157: 1549–1562, 2000.
48. **Xu Y, Clark JC, Aronow BJ, Dey CR, Liu C, Wooldridge JL, Whitsett JA.** Transcriptional adaptation to cystic fibrosis transmembrane conductance regulator deficiency. *J Biol Chem* 278: 7674–7682, 2003.
49. **Yamamoto K, Cox JP, Friedrich T, Christie PT, Bald M, Houtman PN, Lapsley MJ, Patzer L, Tsimaratos M, Van'T Hoff WG, Yamaoka K, Jentsch TJ, Thakker RV.** Characterization of renal chloride channel (CLCN5) mutations in Dent's disease. *J Am Soc Nephrol* 11: 1460–1468, 2000.
50. **Zeeberg BR, Feng W, Wang G, Wang MD, Fojo AT, Sunshine M, Narasimhan S, Kane DW, Reinhold WC, Lababidi S, Bussey KJ, Riss J, Barrett JC, Weinstein JN.** GoMiner: a resource for biological interpretation of genomic and proteomic data. *Genome Biol* 4: R28.1–R28.8, 2003.
51. **Zha X, Genest J Jr, McPherson R.** Endocytosis is enhanced in Tangier fibroblasts: possible role of ATP-binding cassette protein A1 in endosomal vesicular transport. *J Biol Chem* 276: 39476–39483, 2001.
52. **Zhao PL, Wang XT, Zhang XM, Cebotaru V, Cebotaru L, Guo G, Morales M, Guggino SE.** Tubular and cellular localization of the cardiac L-type calcium channel in rat kidney. *Kidney Int* 61: 1393–1406, 2002.